

A binary mixture of spinor atomic Bose-Einstein condensates

Z. F. Xu,¹ Yunbo Zhang,² and L. You^{3,1}

¹Center for Advanced Study, Tsinghua University, Beijing 100084, People's Republic of China

²Institute of Theoretical Physics, Shanxi University, Taiyuan 030006, People's Republic of China

³School of Physics, Georgia Institute of Technology, Atlanta, Georgia 30332, USA

(Dated: November 18, 2018)

We study the ground state and classify its phase diagram for a mixture of two spin-1 condensates in the absence of external magnetic (B-) field according to atomic parameters for intra- and inter-species spin exchange coupling and singlet pairing interaction. Ignoring the inter-species singlet pairing interaction, the ground state phases are found analytically. Numerical approach of simulated annealing is adopted when the singlet pairing interaction is present. Our results on the phase diagram and the boundaries between phases allow for easy identifications of quantum phase transitions, that can be induced through the tuning of optical traps and atom numbers. They provide the first insight and guidance for several ongoing experiments on mixtures of spinor condensates.

PACS numbers: 03.75.Mn, 67.60.Bc, 67.85.Fg, 67.10.-j

The liberation of atomic hyperfine spin from optical trapping opens the study of spin-dependent phenomena in atomic quantum gases [1, 2, 3]. In the simplest case of a spin-1 condensate, two quantum phases: polar and ferromagnetic, exist depending on the sign of atomic spin exchange interaction [4, 5, 6]. The spin-2 system accompanied by richer physics is significantly more complicated as in other higher spin systems [7, 8, 9, 10]. Recently several groups have initiated the study of spin-3 systems, of which the atomic ⁵²Cr is a viable experimental candidate [11, 12]. Parallel to the efforts on spinor condensates are active studies of condensate mixtures with more than one atomic species or state [13, 14, 15, 16, 17, 18, 19]. Earlier works on double condensates rely on atoms with two almost identically trapped internal states [14, 15], while more recent experiments demonstrated mixed condensates with tunable inter-species interactions [20, 21]. Although the field is blossom with extensive studies on spinor condensates and mixtures of scalar condensates, few have touched the subject of mixtures of spinor condensates [22].

This work concerns a binary mixture of spin-1 condensates, with the mixture of ²³Na and ⁸⁷Rb atoms being a special case [22]. We study and identify the ground state phase diagram under the mean-field approximation and the single spatial mode approximation (SMA) for each of the two spinor condensates. Our theory can be extended to more general mixtures of higher spin condensates or mixtures with more than two constituents.

The interaction between two different spin-1 atoms is described by the contact pseudo-potential $V_{12}(\vec{r}_1 - \vec{r}_2) = (g_0^{(12)}\mathcal{P}_0 + g_1^{(12)}\mathcal{P}_1 + g_2^{(12)}\mathcal{P}_2)\delta(\vec{r}_1 - \vec{r}_2)$, where $g_{0,1,2}^{(12)} = 4\pi\hbar^2 a_{0,1,2}^{(12)}/\mu$, $a_{0,1,2}^{(12)}$ are s-wave scattering lengths in the channel of total spin $F_{\text{tot}} = 0, 1, 2$ respectively. μ is the reduced mass. $\mathcal{P}_{0,1,2}$ is the corresponding projection operator. Using $\vec{F}_1 \cdot \vec{F}_2 = \mathcal{P}_2 - \mathcal{P}_1 - 2\mathcal{P}_0$ [4, 5], we find

$$V_{12}(\vec{r}_1 - \vec{r}_2) = (\alpha + \beta\mathbf{F}_1 \cdot \mathbf{F}_2 + \gamma\mathcal{P}_0)\delta(\vec{r}_1 - \vec{r}_2), \quad (1)$$

where $\alpha = (g_1^{(12)} + g_2^{(12)})/2$, $\beta = (-g_1^{(12)} + g_2^{(12)})/2$, and

$\gamma = (2g_0^{(12)} - 3g_1^{(12)} + g_2^{(12)})/2$. Between same species spin-1 atoms, the interaction takes the familiar form $V_{1,2}(\vec{r}_1 - \vec{r}_2) = (\alpha_{1,2} + \beta_{1,2}\mathbf{F}_{1,2} \cdot \mathbf{F}_{1,2})\delta(\vec{r}_1 - \vec{r}_2)$, which respects the identical particle symmetry, thus does not include the odd symmetry term of total spin 1 projection [4, 5].

When atom numbers for both condensates are large, mean-field approximations can be satisfactorily applied. We further assume atomic interaction parameters are such that SMA [6, 23] for each spinor condensate holds, *i.e.*, the mean-field mode functions are almost identical for the three components of each spinor condensate. We thus take $\hat{\Psi}_i(\vec{r}) = \sqrt{N_1}\psi(\vec{r})\zeta_i^{(1)}$ and $\hat{\Phi}_i(\vec{r}) = \sqrt{N_2}\phi(\vec{r})\zeta_i^{(2)}$, respectively, for the mean fields of the two condensates. The mode functions $\psi(\vec{r})$ and $\phi(\vec{r})$, determined presumably by the stronger density dependent interactions, are normalized according to $\int d\vec{r}|\psi(\vec{r})|^2 = \int d\vec{r}|\phi(\vec{r})|^2 = 1$. N_1 and N_2 denote total atom numbers for the two condensates, distributed into the respective spinor component with $N_i^{(1,2)}$ ($\sum_i N_i^{(1,2)} = N_{1,2}$). The effective order parameters for the spinor fields are $\zeta_i^{(1)} = \sqrt{N_i^{(1)}/N_1}e^{-i\theta_i}$ and $\zeta_i^{(2)} = \sqrt{N_i^{(2)}/N_2}e^{-i\varphi_i}$ with θ_i and φ_i real phase values. Neglecting spin-independent terms, the Hamiltonian for our model of a mixture of two spin-1 condensates takes the form

$$H = \frac{1}{2}N_1^2C_1\beta_1\mathbf{f}_1^2 + \frac{1}{2}N_2^2C_2\beta_2\mathbf{f}_2^2 + \frac{1}{2}N_1N_2C_{12}\beta\mathbf{f}_1 \cdot \mathbf{f}_2 + \frac{1}{6}N_1N_2C_{12}\gamma|s_-|^2. \quad (2)$$

The interaction coefficients are $C_1 = \int d\vec{r}|\psi(\vec{r})|^4$, $C_2 = \int d\vec{r}|\phi(\vec{r})|^4$, and $C_{12} = \int d\vec{r}|\psi(\vec{r})|^2|\phi(\vec{r})|^2$. $f_{1i} = \sum_{m,n}\zeta_m^{(1)*}F_{mn}^i\zeta_n^{(1)}$, $f_{2i} = \sum_{m,n}\zeta_m^{(2)*}F_{mn}^i\zeta_n^{(2)}$, and $s_- = \sum_m(-1)^m\zeta_m^{(1)}\zeta_{-m}^{(2)}$. Whether the two condensates are miscible, *i.e.*, completely overlap or not, is unimportant. As long as the SMA holds for each spinor condensate, our model retains its validity even for immiscible condensates with diminishing cross spin coupling $\propto C_{12}$.

Given the interaction coefficients, the above Hamilto-

nian (2) describes a system of two interacting spins. It involves a total of six complex variables when treated semi-classically. The $U(1)$ gauge symmetries for the two condensates give rise to two constraints: the conservation of total atom numbers in each condensate. After a detailed calculation, three independent relative phases appear which we chose as: $\eta_1 = \theta_1 + \theta_{-1} - 2\theta_0$, $\eta_2 = \varphi_1 + \varphi_{-1} - 2\varphi_0$, and $\eta_3 = \theta_{-1} + \varphi_1 - \varphi_{-1} - \theta_1$.

To find the global ground state regardless of magnetization, we minimize Eq. (2) with respect to $N_i^{(1)}$, $N_i^{(2)}$, and the relative phases $\eta_{1,2,3}$ defined above. Alternatively, we can minimize with respect to semi-classical spin variables. Both approaches give the same results, provided that $\zeta_i^{(1,2)}$ is replaced by the normalized value $\zeta_i^{(1,2)}/\sqrt{\sum_i N_i^{(1,2)}/N_{1,2}}$ to take into account the constraints explicitly. The multi-dimensional minimization is numerically carried out with the method of simulated annealing [24] where analytical approach fails. Without loss of generality, we report the special case of $N_1 = N_2 = N$ in the following.

We first discuss the simple situation of $\gamma = 0$. The results will serve as reference states for the complete ground state phase diagram. As the ground state is degenerate, it is convenient to restrict into the subspace of $f_{i+} = f_{i-} = 0$ ($i = 1, 2$), which leaves two unknowns: f_{1z} and f_{2z} . The ground state is analytically derived including explicit formulae for phase boundaries as functions of spin coupling parameters. Figure 1 illustrates the dependence of order parameters on the inter-species interaction $C_{12}\beta$ at fixed values of intra-species spin exchange interaction parameter $C_1\beta_1$ and $C_2\beta_2$, which categorize the ground state into three cases.

First, when the two spin-1 condensates are both ferromagnetic, the ground state is simple, as shown in Fig. 1(a). Both spins are polarized: $\mathbf{f}_1^2 = \mathbf{f}_2^2 = 1$. When $C_{12}\beta > 0$, they are anti-aligned as $\mathbf{f}_1 \cdot \mathbf{f}_2 = -1$. When $C_{12}\beta < 0$, they are aligned with $\mathbf{f}_1 \cdot \mathbf{f}_2 = 1$.

Secondly when both condensates are polar with $C_1\beta_1 > 0$ and $C_2\beta_2 > 0$, we assume $C_1\beta_1 \neq C_2\beta_2$ without loss of generality. The ground state is found to exhibit several phases. If $C_{12}|\beta| < 2\sqrt{C_1\beta_1 C_2\beta_2}$, *i.e.*, for weak intra-species spin exchange interaction, the two spins become essentially independent, giving rise to $\mathbf{f}_1^2 = 0$, $\mathbf{f}_2^2 = 0$, and $\mathbf{f}_1 \cdot \mathbf{f}_2 = 0$. With increasing strength of $C_{12}|\beta|$, one of the spins become polarized and the other is partially polarized for $2\sqrt{C_1\beta_1 C_2\beta_2} < C_{12}|\beta| < 2\max(C_1\beta_1, C_2\beta_2)$. The exact value for the resulting partial polarization is determined by the relative strengths of the two intra-species spin-exchange interactions. For $C_1\beta_1 < C_2\beta_2$, we have $\mathbf{f}_1^2 = 1$, $\mathbf{f}_2^2 = (C_{12}\beta/2C_2\beta_2)^2$, and $\mathbf{f}_1 \cdot \mathbf{f}_2 = -C_{12}\beta/2C_2\beta_2$. At stronger inter-species spin exchange interaction, when $C_{12}|\beta| > 2\max(C_1\beta_1, C_2\beta_2)$, the spin-spin coupling between the two condensates causes all atoms to be polarized as illustrated in Fig. 1(b).

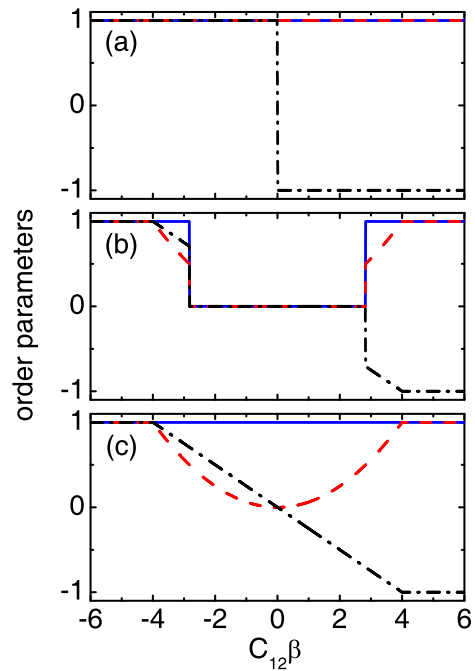


FIG. 1: (Color online). The dependence of ground state order parameters on $C_{12}\beta$ at fixed values of $C_1\beta_1$ and $C_2\beta_2$, for $\gamma = 0$. Blue solid lines, red dashed lines, and black dot-dashed lines denote respectively the mean field order parameters \mathbf{f}_1^2 , \mathbf{f}_2^2 , and $\mathbf{f}_1 \cdot \mathbf{f}_2$. The three subplots refer to the three cases of fixed intra-species spin exchange interactions $(C_1\beta_1, C_2\beta_2) =$: (a) $(-1, -2)$; (b) $(1, 2)$; and (c) $(-1, 2)$.

The third case as shown in Fig. 1(c), with one ferromagnetic ($C_1\beta_1 < 0$) and one polar condensate ($C_2\beta_2 > 0$), is found to be similar to case (b) of two polar condensates. When $C_{12}|\beta| < 2\max(C_1\beta_1, C_2\beta_2)$, the ground state gives $\mathbf{f}_1^2 = 1$, $\mathbf{f}_2^2 = (C_{12}\beta/2C_2\beta_2)^2$, and $\mathbf{f}_1 \cdot \mathbf{f}_2 = -C_{12}\beta/2C_2\beta_2$, which is the same as in case (b). When $C_{12}|\beta| > 2\max(C_1\beta_1, C_2\beta_2)$, we find $\mathbf{f}_1^2 = 1$, $\mathbf{f}_2^2 = 1$, and $|\mathbf{f}_1 \cdot \mathbf{f}_2| = 1$. We note that Luo *et al.* [22], recently performed quantum calculations and studied the energy band structure of essentially the same model for this case using estimated inter-species atomic parameters for ^{87}Rb and ^{23}Na atoms [25, 26].

Next, we discuss the general case of $\gamma \neq 0$. Before considering the full Hamiltonian (2), we illustrate the phase diagram for the special case of $C_1\beta_1 = C_2\beta_2 = 0$ in Fig. 2. Only two terms remain in the Hamiltonian, which formally resembles the Hamiltonian of a spin-2 condensate [8]. The phases PP, FF, CC, and AA are characterized by the two order parameters $(\mathbf{f}_1 \cdot \mathbf{f}_2 = 0, |s_-| = 1)$, $(\mathbf{f}_1 \cdot \mathbf{f}_2 = 1, |s_-| = 1)$, $(\mathbf{f}_1 \cdot \mathbf{f}_2 = 0, |s_-| = 0)$, and $(\mathbf{f}_1 \cdot \mathbf{f}_2 = -1, |s_-| = 1)$, respectively. The other two order parameters take fixed values $(\mathbf{f}_1^2 = 0, \mathbf{f}_2^2 = 0)$, $(\mathbf{f}_1^2 = 1, \mathbf{f}_2^2 = 1)$, and $(\mathbf{f}_1^2 = 1, \mathbf{f}_2^2 = 1)$ respectively in the PP, FF, and AA phases, while for the CC phase, their values remain undetermined. Compared to a spin-2 condensate, we find the PP, FF, and CC phases are similar to the polar, ferromagnetic, and cyclic phases respectively. There exists

no counterpart for the AA phase in a spin-2 condensate. The two hypothetical (spin-1) sub-spins \mathbf{f}_1 and \mathbf{f}_2 making up the total spin-2 are constrained to be identical. In the case of a mixture as we discuss here, however, the two spins are different. The phase boundaries are specified by two lines with $\beta = 0$ and $3\beta = \gamma$ as in a spin-2 condensate. The transitions between different phases are all first order in this case.

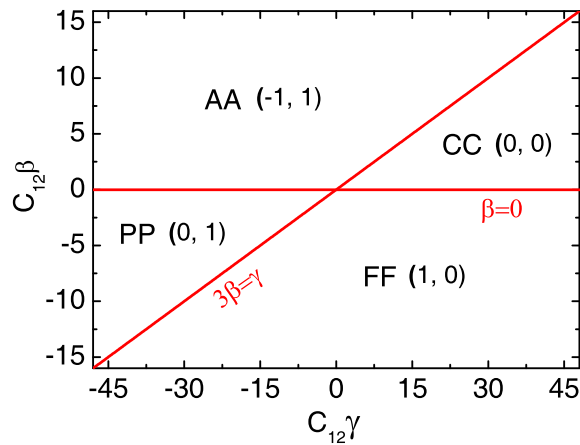


FIG. 2: (Color online). The ground state phase diagram for our model when only inter-species spin exchange and singlet pair pairing interactions are present. Red solid lines denote discontinuous phase transition boundaries. The PP, FF, CC, and AA phases are denoted by the values for the two order parameters $(\mathbf{f}_1 \cdot \mathbf{f}_2, |s_-|) = (0, 1), (1, 0), (0, 0),$ and $(-1, 1)$ respectively.

The most general case of our model Hamiltonian (2) is when all terms are present. As before for $\gamma = 0$, we will restrict to respective cases specified by the fixed values for $C_1\beta_1$ and $C_2\beta_2$. Using full numerical simulations, we find the dependence of ground state phases on the four parameters: $C_1\beta_1, C_2\beta_2, C_{12}\beta,$ and $C_{12}\gamma$. The competitions among the first three determine the ground state as categorized in Fig. 1. The γ -term encourages pairing two different type of atoms into singlets when $\gamma < 0$; it minimizes $|s_-|$ instead when $\gamma > 0$. If $C_{12}|\gamma|$ is small enough compared to the first three parameters, then intuitively we expect the ground state structure of Fig. 1 will largely remain intact. However, our numerical results uncover remarkable differences between $\gamma > 0$ and $\gamma < 0$ even when its value is small. In the extreme circumstance when $C_{12}|\beta| \gg 1$ and $C_{12}|\gamma| \gg 1$, the ground state is fully determined by the respective ratio of β to γ , resulting in the same phase diagram as for $C_1\beta_1 = C_2\beta_2 = 0$, which is illustrated in Fig. 2. The resulting phases are categorized as before and illustrated in Fig. 3.

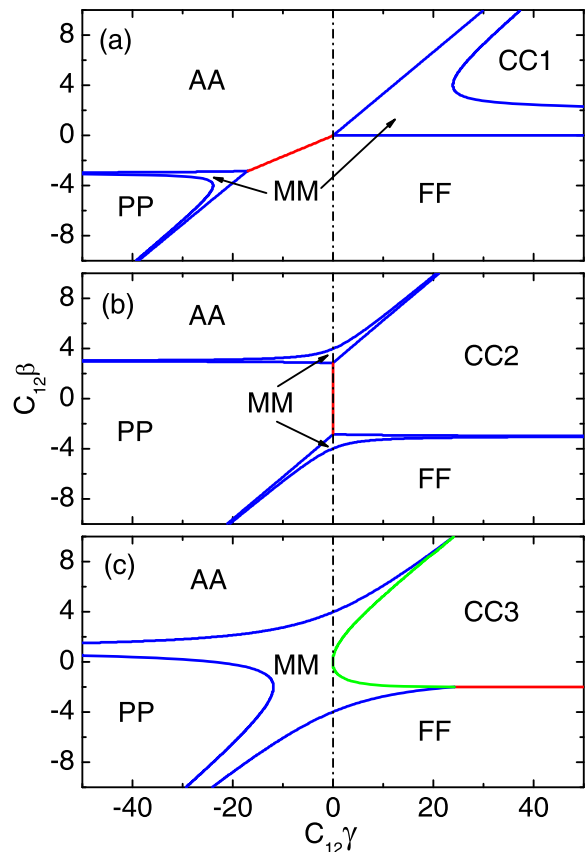


FIG. 3: (Color online). The ground state phase diagram of our model at fixed values of $C_1\beta_1, C_2\beta_2$. Blue solid lines denote continuous phase transition boundaries. Red solid lines denote discontinuous phase transition boundaries between two phases with fully determined order parameters. The green solid line denotes the discontinuous phase transition boundary between the fully determined phase CC3 and the MM phase. The black dash-dotted lines correspond to $C_{12}\gamma = 0$, which serve as guides for the eye. The three subplots denote fixed intra-species spin exchange interaction parameters as in Fig. 1, $(C_1\beta_1, C_2\beta_2) =$: (a) $(-1, -2)$; (b) $(1, 2)$; and (c) $(-1, 2)$.

First, for two ferromagnetic condensates, corresponding to Fig. 1(a) of $C_{12}\gamma = 0$, we find two phases: AA and FF for $C_{12}\beta > 0$ and $C_{12}\beta < 0$ respectively. The phase transition between them are discontinuous. Increasing $C_{12}\gamma$ along the negative axis direction, we find the same two phases AA and FF if $C_{12}|\gamma|$ remains small in value, although the phase boundary is found to shift with changing $C_{12}|\gamma|$. Further increasing the strength of singlet pairing interaction, a new phase MM emerges between the AA and FF phases, where all four order parameters evolve continuously to border the AA and FF phases. Beyond a critical value of $C_{12}|\gamma|$, the PP phase occupies an interval section of the parameter $C_{12}\beta$. Next, we increase $C_{12}\gamma$ from 0 along the positive axis direction. In the beginning, a positive γ -term decreases $|s_-|$. No matter how small $C_{12}|\gamma|$ is, the critical point (at $\gamma = 0$) between the phases AA and FF diffuses into an interval,

and all four order parameters change continuously from the FF to the AA phase. When $C_{12}\gamma$ is sufficiently large, as in the case of the opposite direction when $C_{12}\gamma < 0$, a special type of CC phase, which we call CC1 ($\mathbf{f}_1^2 = 0$, $\mathbf{f}_2^2 = 1$) arises over an interval of the parameter $C_{12}\beta$. A continuous transition region is found to surround the CC1 phase and borders the FF and AA phases. These results are summarized in Fig. 3(a), with the boundaries of continuous (discontinuous) phase transitions denoted by blue (red) solid lines.

The case of two polar condensates ($0 < C_1\beta_1 < C_2\beta_2$) are shown in Fig. 3(b). The $C_{12}\gamma = 0$ line is seen to be partitioned into five intervals. The middle interval around $C_{12}\beta = 0$ is the region where the two spins are completely independent as discussed before. Additionally, two continuous changing intervals belong to the MM phase. The remaining two intervals are the AA and FF phases, the same as in the first case of Fig. 3(a). The inclusion of the fourth competing interaction γ -term, we find a new phase emerges on each side of the $C_{12}\gamma = 0$ line irrespective of the value of the γ -term. This confirms the middle interval is really a boundary between the PP phase and a second special type of CC phase, denoted as CC2 ($\mathbf{f}_1^2 = 0$, $\mathbf{f}_2^2 = 0$). The transition across is found to be discontinuous. When $C_{12}\gamma < 0$, the PP phase is found to dominate. In the opposite case, the CC2 phase wins.

The third case corresponds to a mixture of one ferromagnetic ($C_1\beta_1 < 0$) and one polar ($C_2\beta_2 > 0$) condensate. When $C_{12}\gamma = 0$ as discussed before, there exist two phases AA and FF in both sides of the $C_{12}\beta$ axis, plus a middle continuous transition region. When $C_{12}\gamma \neq 0$, we first decrease $C_{12}\gamma$ along the negative axis from 0. Before reaching a critical value, the ground state phase is found to be essentially the same as for $C_{12}\gamma = 0$. Beyond this critical value, a PP phase emerges as in the first case of Fig. 3(a). Increasing $C_{12}\gamma \neq 0$ along the positive axis, the results is found to change completely. The critical value disappears. A third type of CC phase, labeled as CC3 ($\mathbf{f}_1^2 = 1$, $\mathbf{f}_2^2 = 0$), emerges in the middle region. The transition between the CC3 and the middle transition region MM phase is discontinuous on both boundaries along the axis of $C_{12}\beta$, denoted as green solid lines in Fig. 3(c). This discontinuous phase transition boundary is distinct from that of the red solid lines, which denote boundaries between two phases with fixed order parameters and the changes for all four order parameters across the boundaries are exactly known.

Finally we hope to point out that although inter-species interaction parameters are fixed, the interaction coefficients in the model we consider such as $C_{12}\beta$ and $C_{12}\gamma$ remain tunable by controlling optical trapping potentials or adjusting atom numbers. In this study, we consider the special case of two equally populated condensates inside fixed traps. In reality the effect of different atom numbers can be used to adjust the four interaction coefficients. We can also use different optical traps for the two species of atoms, which can further enhance

the tunability of the different ranges and ratios of the values for C_1 , C_2 , and C_{12} .

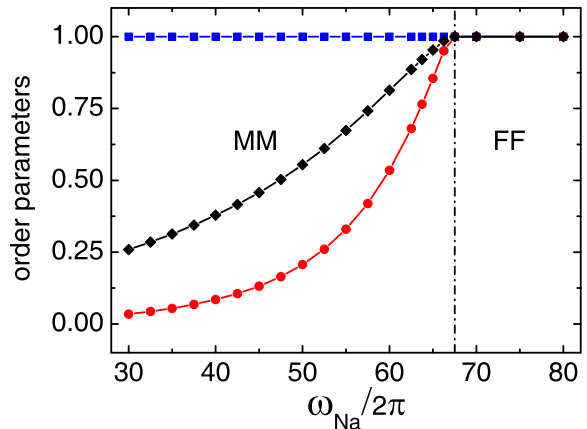


FIG. 4: (Color online). The dependence of the ground state order parameters on the trap frequency ω_{Na} , at a fixed $\omega_{\text{Rb}} = 2\pi \times 50\text{Hz}$. Blue squares, red circles, and black diamonds denote respectively for the three order parameter \mathbf{f}_1^2 , \mathbf{f}_2^2 , and $\mathbf{f}_1 \cdot \mathbf{f}_2$. Lines are guides for the eye obtained from connecting neighbouring data points. Dot-dashed line specifies the phase boundary between the MM and the FF phase.

As a concrete example, we consider here a realizable experiment to demonstrate a quantum phase transition from the MM phase to the FF phase in a binary mixture of ^{87}Rb (species one) and ^{23}Na (species two) spin-1 condensates. The tuning is achieved through the control of the trapping frequency for Na atoms. We assume 5×10^5 ^{87}Rb atoms and 10^5 ^{23}Na atoms are confined harmonically $V_a(\vec{r}) = \frac{1}{2}M_a\omega_a r^2$ with $\omega_{\text{Rb}} = 2\pi \times 50\text{Hz}$, and ω_{Na} tunable from $2\pi \times 30$ to $2\pi \times 80\text{Hz}$. The inter-species atomic parameters between ^{87}Rb and ^{23}Na are unknown. We therefore resort to the simple approach of degenerate internal states [25, 26, 27] as the low energy atomic interactions can be mostly attributed to the ground state configurations of the two valence electrons. The inter-species scattering lengths for singlet and triplet electronic states are approximately determined already, given by $a_S = 109a_0$ and $a_T = 70a_0$ [25, 26], where a_0 is the Bohr radius. The inter-species interactions between ^{87}Rb and ^{23}Na atoms are then parameterized by three scattering lengths, each being a linear combination of a_S and a_T weighted by the appropriate $9j$ coefficients for the total combined spins of $F_{\text{tot}} = 0, 1$, and 2 [22]. Within this approximation, it's found coincidentally [22] that γ , the parameter for inter-species singlet pairing interaction is equal to zero. The ground states are found through imaginary-time propagation of the corresponding coupled Gross-Pitaevskii equations. To compare with our former results within SMA, we redefine the three order parameters as $\mathbf{f}_1^2 = \int d\vec{r}(\psi_i^* \vec{F}_{ij} \psi_j)^2 / \int d\vec{r}(\psi_i^* \psi_i)^2$, $\mathbf{f}_2^2 = \int d\vec{r}(\phi_i^* \vec{F}_{ij} \phi_j)^2 / \int d\vec{r}(\phi_i^* \phi_i)^2$, and $\mathbf{f}_1 \cdot \mathbf{f}_2 = \int d\vec{r}(\psi_i^* \vec{F}_{ij} \psi_j) \cdot (\phi_i^* \vec{F}_{ij} \phi_j) / \int d\vec{r}(\psi_i^* \psi_i)(\phi_i^* \phi_i)$, where ψ_i and ϕ_i ($i = 1, 0, -1$) are component wave functions respectively for

^{87}Rb and ^{23}Na condensates. When the SMA is satisfied, they reduce to that as defined in Eq. (2), and the values of the order parameters become the same as in Fig. 1(c). This is indeed the case for most of our numerical calculations, especially in the FF phase, with all atoms fully spin polarized, or when two condensates are uncorrelated.

In Fig. 4, the three order parameters for the ground state are demonstrated under the changing trapping frequency of ^{23}Na atoms. With increasing value of ω_{Na} , the ferromagnetic spin-spin coupling between ^{87}Rb and ^{23}Na atoms will induce the spin polarization of ^{23}Na atoms, from initially unpolarized to a full polarization. Compared to the phase diagram of a mixture with one ferromagnetic and one polar spin-1 condensate as in Fig. 3(c), it's clear that by tuning the trap frequency for the ^{23}Na condensate, we induce a quantum phase transition from the MM phase to the FF phase in the mixture.

To conclude, we study the ground state of a binary mixture of two spin-1 condensates in the absence of B-field, using both analytical approaches and the numeri-

cal method of simulated annealing. Neglecting the singlet pairing interaction between the two species of atoms ($\gamma = 0$), we present analytical formulae for all order parameters of the ground state phase diagram including all phase boundaries and the development of order parameters. When $\gamma \neq 0$, we find the phase diagram for the ground state at three groups of specific values for the intra-species spin coupling interactions. We suggest it is possible to tune to different phases, or induce quantum phase transitions by changing optical traps and/or atom numbers in the two condensates respectively. Finally, we confirm that the mean field theory we adopt remains an excellent approximation as all our results have been repeated numerically with the full quantum approach of exact diagonalization at small atom numbers.

This work is supported by US NSF, NSF of China under Grant 10640420151 and 10774095, and NKBRF of China under Grants 2006CB921206, 2006AA06Z104 and 2006CB921102.

-
- [1] D. M. Stamper-Kurn, M. R. Andrews, A. P. Chikkatur, S. Inouye, H.-J. Miesner, J. Stenger, and W. Ketterle, *Phys. Rev. Lett.* **80**, 2027 (1998).
- [2] J. Stenger *et al.*, *Nature (London)* **396**, 345 (1998).
- [3] M. Barrett, J. Sauer, and M. S. Chapman, *Phys. Rev. Lett.* **87**, 010404 (2001).
- [4] Tin-Lun Ho, *Phys. Rev. Lett.* **81**, 742 (1998).
- [5] T. Ohmi and K. Machida, *J. Phys. Soc. Jpn.* **67**, 1822 (1998).
- [6] C. K. Law, H. Pu, and N. P. Bigelow, *Phys. Rev. Lett.* **81**, 5257 (1998).
- [7] Masato Koashi and Masahito Ueda, *Phys. Rev. Lett.* **84**, 1066 (2000).
- [8] C. V. Ciobanu, S.-K. Yip, and Tin-Lun Ho, *Phys. Rev. A* **61**, 033607 (2000).
- [9] M. Ueda and M. Koashi, *Phys. Rev. A* **65**, 063602 (2002).
- [10] Ryan Barnett, Ari Turner, and Eugene Demler, *Phys. Rev. Lett.* **97**, 180412 (2006).
- [11] L. Santos and T. Pfau, *Phys. Rev. Lett.* **96**, 190404 (2006).
- [12] R. B. Diener and Tin-Lun Ho, *Phys. Rev. Lett.* **96**, 190405 (2006).
- [13] Tin-Lun Ho and V. B. Shenoy, *Phys. Rev. Lett.* **77**, 3276 (1996).
- [14] C. J. Myatt, E. A. Burt, R. W. Ghrist, E. A. Cornell, and C. E. Wieman, *Phys. Rev. Lett.* **78**, 586 (1997).
- [15] D. S. Hall, M. R. Matthews, J. R. Ensher, C. E. Wieman, and E. A. Cornell, *Phys. Rev. Lett.* **81**, 1539 (1998).
- [16] H. Pu and N. P. Bigelow, *Phys. Rev. Lett.* **80**, 1130 (1998).
- [17] E. Timmermans, *Phys. Rev. Lett.* **81**, 5718 (1998).
- [18] B. D. Esry and C. H. Greene, *Nature* **392**, 434 (1998).
- [19] G. Modugno, M. Modugno, F. Riboli, G. Roati, and M. Inguscio, *Phys. Rev. Lett.* **89**, 190404 (2002).
- [20] G. Thalhammer, G. Barontini, L. De Sarlo, J. Catani, F. Minardi, and M. Inguscio, *Phys. Rev. Lett.* **100**, 210402 (2008).
- [21] S. B. Papp, J. M. Pino, and C. E. Wieman, *Phys. Rev. Lett.* **101**, 040402 (2008).
- [22] Ma Luo, Zhibing Li, and Chengguang Bao, *Phys. Rev. A* **75**, 043609 (2007).
- [23] S. Yi, Ö. E. Müstecaplıoğlu, C. P. Sun, and L. You, *Phys. Rev. A* **66**, 011601(R) (2002).
- [24] S. Kirkpatrick, C. D. Gelatt, and M. P. Vecchi, *Science* **220**, 671 (1983).
- [25] S. B. Weiss, M. Bhattacharya, and N. P. Bigelow, *Phys. Rev. A* **68**, 042708 (2003).
- [26] A. Pashov, O. Docenko, M. Tamanis, R. Ferber, H. Knöckel, and E. Tiemann, *Phys. Rev. A* **72**, 062505 (2005).
- [27] H. T. Stoof, J. M. Koelman, and B. J. Verhaar, *Phys. Rev. B* **38**, 4688 (1988).